

# Tau Decays into Hadrons

The  $\tau$  lepton is an elementary particle with spin  $1/2$  and as mass of  $1.776\,86\text{ GeV}$  [PDG2018]. It is the only lepton heavy enough to decay into hadrons but also light enough for performing a low-energy QCD analysis. Its inclusive hadronic<sup>1</sup> decay ratio is given by

$$R_\tau = \frac{\Gamma(\tau \rightarrow \nu_\tau + \text{hadrons})}{\Gamma(\tau \rightarrow \nu_\tau e^+ e^-)} \quad (1.0.1)$$

and sensible to the strong coupling, due to its rather large value, at the  $m_\tau^2$  scale, of approximately 0.33. On the other hand  $\alpha_s(m_\tau^2)$  is small enough to apply the OPE. The NP OPE contributions to the decay ratio are suppressed. The dimension two contribution of the OPE is proportional to the quark masses and has only a tiny contribution for light quarks. The dimension four contribution can be suppressed by applying weight functions, that do not have a monomial in  $x$ . E.g. the kinematic weight  $\omega_\tau = (1-x)^2(1+2x) = 1 - 3x^2 + 2x^3$  is not sensitive to OPE corrections of dimension four. Also the apparent DV in  $\tau$  hadronic decays can be suppressed by applying pinched weights. The dimension six contribution of the OPE is proportional to  $1/(m_\tau^2)^3$  and further suppressed in the V+A channel as the vector and axial-vector  $D = 6$  contributions have opposite signs and cancel themselves. Higher dimensional OPE contributions are suppressed by terms  $1/m_\tau^n$  with  $n \geq 8$ . As a result the perturbative contributions are dominant. They are known up to  $(\alpha_s^4)$  with a total contribution of 20% [Pich2016a], which enables us to perform precise calculations of the inclusive  $\tau$  decay ratio. Furthermore by extracting  $\alpha_s$  at low energies at the scale of  $m_\tau^2$  we will achieve lower errors for the strong coupling at higher energies as the

---

<sup>1</sup>Meaning all decay channels with a hadron in its final state.

errors run with the strong coupling and get smaller with increasing energy.

Summarising the  $\tau$  decays permit one of the most precise determinations of the strong coupling  $\alpha_s$ . Building on the previously presented QCDSR we will now elaborate the needed theory to extract  $\alpha_s$  from the process of hadronic tau decays.

## 1.1 The Inclusive Decay Ratio

The theoretical expression of the inclusive hadronic decay ratio (eq. 1.0.1) is given by

$$R_\tau(s) = 12\pi S_{EW}|V_{ud}|^2 \int_0^{m_\tau} \frac{ds}{m_\tau^2} \left(1 - \frac{s}{m_\tau^2}\right) \left[ \left(1 + 2\frac{s}{m_\tau^2}\right) \text{Im} \Pi^{(1)}(s) + \text{Im} \Pi^{(0)}(s) \right], \quad (1.1.1)$$

where  $S_{EW}$  is the electro-weak correction,  $V_{ud}$  the corresponding *Cabibbo-Kobayashi-Maskawa* (CKM) matrix element and  $\text{Im} \Pi$  the imaginary part of the two-point function we introduced in ?? . For brevity we will omit the electro-weak  $S_{EW}$  and CKM factors from now on. Equation 1.1.1 was first derived by [Tsai1971], using current algebra, a more recent derivation making use of the *optical theorem*, as already mentioned in ?? can be taken from [Schwab2002]. Notice that we used the standard lorentz decomposition into transversal ( $J = 1$ ) and longitudinal ( $J = 0$ ) components of ?? to display the hadronic decay ratio (eq. 1.1.1). Applying Cauchy's theorem, as seen in ??, to the eq. 1.1.1 we can rewrite the line integral into a closed contour integral

$$R_\tau = 6\pi i \oint_{|s|=m_\tau} \frac{ds}{m_\tau^2} \left(1 - \frac{s}{m_\tau^2}\right) \left[ \left(1 + 2\frac{s}{m_\tau^2}\right) \Pi^{(1)}(s) + \Pi^{(0)}(s) \right]. \quad (1.1.2)$$

It is convenient to work with a slightly different combination of transversal and longitudinal components  $\Pi^{(1+0)}$ , which has been defined in ?? and is free of kinematic singularities. As a result we can further rewrite the hadronic  $\tau$  decay ratio into

$$R_\tau = 6\pi i \oint_{|s|=m_\tau} \frac{ds}{m_\tau^2} \left(1 - \frac{s}{m_\tau^2}\right)^2 \left[ \left(1 + 2\frac{s}{m_\tau^2}\right) \Pi^{(1+0)}(s) - \left(\frac{2s}{m_\tau^2}\right) \Pi^{(0)}(s) \right]. \quad (1.1.3)$$

In the case of  $\tau$  decays we only have to consider vector and axial-vector contributions of decays into up, down and strange quarks. Thus taking  $i, j$  as the

flavour indices for the light quarks (u, d and s) we can express the two-point function as

$$\Pi_{\mu\nu,ij}^{V/A}(s) \equiv i \int dx e^{ipx} \langle \Omega | T \{ J_{\mu,ij}^{V/A}(x) J_{\nu,ij}^{V/A}(0)^\dagger \} | \Omega \rangle, \quad (1.1.4)$$

with  $|\Omega\rangle$  being the physical vacuum. The vector and axial-vector currents are then distinguished by the corresponding dirac-matrices ( $\gamma_\mu$  and  $\gamma_\mu\gamma_5$ ) given by

$$J_{\mu,ij}^V(x) = \bar{q}_j(x) \gamma_\mu q_i(x) \quad \text{and} \quad J_{\mu,ij}^A(x) = \bar{q}_j(x) \gamma_\mu \gamma_5 q_i(x). \quad (1.1.5)$$

With [eq. 1.1.3](#) we have a suitable physical quantity that can be theoretically calculated as experimentally measured. By using the QCDSR we apply a closed contour integral of radius  $s_0$ . As a result we successfully avoided low energies at which the application of PT would be questionable. For example if we would choose a radius with the size of the  $\tau$  mass  $m_\tau \approx 1.78 \text{ MeV}$  the strong coupling would have a perturbatively safe value of  $\alpha_s(m_\tau^2) \approx 0.33$  [Pich2016]. Obviously we would benefit even more from a contour integral over a bigger circumference, but  $\tau$  decays are kinematically limited by their mass. Nevertheless there are promising  $e^+e^-$  annihilation data, which yield valuable inclusive decay ratio values up to 2 GeV [Boito2018][Keshavarzi2018].

### 1.1.1 Renormalisation Group Invariance

We have seen in ??, that the two-point function is not a physical quantity, as the dispersion relation (??) contains a unphysical polynom. Luckily for the vector correlator, appearing in hadronic tau decays, the polynom is just a constant. Consequently we can take the derivative with respect to the momentum  $s$  to derive a physical quantity from the two-point function:

$$D(s) \equiv -s \frac{d}{ds} \Pi(s). \quad (1.1.6)$$

$D(s)$  is called the *Adler function* and fulfils, as all physical quantities, the RGE (??). The Adler function commonly has separate definitions for the longitudinal plus transversal and the solely longitudinal contributions:

$$D^{(1+0)}(s) \equiv -s \frac{d}{ds} \Pi^{(1+0)}(s), \quad D^{(0)}(s) \equiv \frac{s}{m_\tau^2} \frac{d}{ds} (s \Pi^{(0)}(s)). \quad (1.1.7)$$

The two-point functions in ?? can now be replaced with the help of partial integration

$$\int_a^b u(x)V(x) dx = [U(x)V(x)]_a^b - \int_a^b U(x)v(x) dx. \quad (1.1.8)$$

We will perform two separate the computations the two cases  $(1+0)$  and  $(0)$ . Starting by the transversal plus longitudinal contribution we get:

$$\begin{aligned} R_\tau^{(1)} &= \frac{6\pi i}{m_\tau^2} \oint_{|s|=m_\tau^2} \underbrace{\left(1 - \frac{s}{m_\tau^2}\right)^2}_{=u(x)} \underbrace{\left(1 + 2\frac{s}{m_\tau^2}\right) \Pi^{(1+0)}(s)}_{=V(x)} \\ &= \frac{6\pi i}{m_\tau^2} \left\{ \left[ -\frac{m_\tau^2}{2} \left(1 - \frac{s}{m_\tau^2}\right)^3 \left(1 + \frac{s}{m_\tau^2}\right) \Pi^{(1+0)}(s) \right]_{|s|=m_\tau^2} \right. \\ &\quad \left. + \oint_{|s|=m_\tau^2} \underbrace{-\frac{m_\tau^2}{2} \left(1 - \frac{s}{m_\tau^2}\right)^3}_{=U(x)} \underbrace{\left(1 + \frac{s}{m_\tau^2}\right) \frac{d}{ds} \Pi^{(1+0)}(s)}_{=v(x)} \right\} \\ &= -3\pi i \oint_{|s|=m_\tau^2} \frac{ds}{s} \left(1 - \frac{s}{m_\tau^2}\right)^3 \left(1 + \frac{s}{m_\tau^2}\right) \frac{d}{ds} D^{(1+0)}(s) \end{aligned} \quad (1.1.9)$$

where we fixed the integration constant to  $c = -\frac{m_\tau^2}{2}$  in the second line and left the antiderivatives contained in the squared brackets untouched. If we parametrise the integral appearing in the expression in the squared brackets we can see that it vanishes:

$$\left[ -\frac{m_\tau^2}{2} \left(1 - e^{-i\phi}\right)^3 \left(1 + e^{-i\phi}\right) \Pi^{(L+T)}(m_\tau^2 e^{-i\phi}) \right]_0^{2\pi} = 0, \quad (1.1.10)$$

where  $s \rightarrow m_\tau^2 e^{-i\phi}$  and  $(1 - e^{-i \cdot 0}) = (1 - e^{-i \cdot 2\pi}) = 0$ . Repeating the same calculation for the longitudinal part yields

$$\begin{aligned} R_\tau^{(0)} &= \oint_{|s|=m_\tau^2} ds \left(1 - \frac{s}{m_\tau^2}\right)^2 \left(-\frac{2s}{m_\tau^2}\right) \Pi^{(0)}(s) \\ &= -4\pi i \oint \frac{ds}{s} \left(1 - \frac{s}{m_\tau^2}\right)^3 D^{(0)}(s) \end{aligned} \quad (1.1.11)$$

Consequently combining the transversal with the longitudinal contribution results in

$$R_\tau = -\pi i \oint_{|s|=m_\tau^2} \frac{ds}{s} \left(1 - \frac{s}{m_\tau^2}\right)^3 \left[ 3 \left(1 + \frac{s}{m_\tau^2}\right) D^{(1+0)}(s) + 4 D^{(0)}(s) \right]. \quad (1.1.12)$$

It is convenient to define  $x = s/m_\tau^2$  such that we can rewrite the inclusive ratio as

$$R_\tau = -\pi i \oint_{|s|=m_\tau^2} \frac{dx}{x} (1-x)^3 \left[ 3(1+x) D^{(1+0)}(m_\tau^2 x) + 4 D^{(0)}(m_\tau^2 x) \right], \quad (1.1.13)$$

which will be the final expression we will be using to express the inclusive tau decay ratio.

## 1.2 Theoretical computation of $R_\tau$

The previously derived expression for the tau decay ratio is at first approximation equal to the number of colours [Peskin1995]

$$R_\tau \approx N_c. \quad (1.2.1)$$

If we take into account the perturbative  $\delta_{pt}$  and non-perturbative  $\delta_{npt}$  we can organise the vector and axial-vector inclusive decay ratio as

$$R_{\tau,V/A}^\omega = \frac{N_c}{2} \left( 1 + \delta_{pt}^\omega + \delta_{npt}^\omega \right). \quad (1.2.2)$$

Note that the factor  $1/2$  comes from the fact, that in the chiral limit the vector and axial-vector contributions are equal. The dependence on the chosen weight function  $\omega$  is reflected in the upper indices.

For the kinematic weight

$$\omega_\tau \equiv (1-x)^2(1+2x), \quad (1.2.3)$$

we have a dominant perturbative contribution of  $\delta_{pt} \approx 20\%$  [Pich2013] and a minor, but not negligible, non-perturbative contribution of  $\delta_{npt} = -0.007 \pm 0.004$  [Braaten1991].

In the following we want to derive the theoretical expressions needed to calculate both of the corrections to eq. 1.2.2 starting with the perturbative one.

### 1.2.1 The perturbative contribution

The perturbative contribution  $\delta_{pt}$  to the inclusive  $\tau$  decay ratio corresponds to the first term of the OPE. Currently the perturbative expansion has been

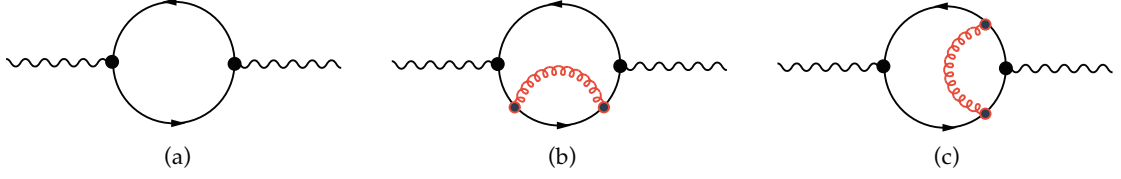


Figure 1.1: Feynman loop diagrams to calculate the  $c_{n,k}$  coefficients of the expanded correlator  $\Pi_V^{(1+0)}$ . The internal red lines represent gluons. Diagram a) represents the parton model and diagrams b) and c) represent higher order corrections.

calculated to fourth order  $\mathcal{O}(\alpha_s^4)$ . Due to their role as dominant corrections their uncertainties from unknown higher-order corrections dictate the final error of the determination of the strong coupling [Pich2016].

We will treat the correlator in the chiral limit, in which the scalar and pseudo-scalar contribution of the two-point function vanish and the axial and vectorial contributions are equal. As a result we can focus ourselves on the vector correlator  $\Pi_V(s)$ , which can be expanded as a sum over different orders of  $\alpha$  [Beneke2008]:

$$\Pi_V^{(1+0)}(s) = -\frac{N_c}{12\pi^2} \sum_{n=0}^{\infty} a_\mu^n \sum_{k=0}^{n+1} c_{n,k} L^k \quad \text{with} \quad L \equiv \ln \frac{-s}{\mu^2}, \quad (1.2.4)$$

where we defined  $a_\mu \equiv \alpha(\mu)/\pi$ . The coefficient  $c_{n,k}$  up to two-loop order can be obtained by Feynman diagram calculations. With the diagrams of fig. 1.1 we can calculate the zero-loop result of the correlator [Jamin2006]

$$\Pi_{\mu\nu}^B(q^2) \Big|^{1\text{-loop}} = \frac{N_c}{12\pi^2} \left( \frac{1}{\hat{\epsilon}} - \log \frac{(-q^2 - i0)}{\mu^2} + \frac{5}{3} + \mathcal{O}(\epsilon) \right), \quad (1.2.5)$$

where  $\Pi_{\mu\nu}^B(q^2)$  is the bare two-point function and is not renormalised<sup>2</sup>. This result can then be used to extract the first two coefficients of the correlator expansion given in eq. 1.2.4

$$c_{00} = -\frac{5}{3} \quad \text{and} \quad c_{01} = 1. \quad (1.2.6)$$

The second loop can also be calculated by diagram techniques resulting in [Boito2011]

$$\Pi_V^{(1+0)}(s) \Big|^{2\text{-loop}} = -\frac{N_c}{12\pi^2} a_\mu \log\left(\frac{-s}{\mu^2}\right) + \dots \quad (1.2.7)$$

<sup>2</sup>The term  $1/\hat{\epsilon}$ , which is of order zero in  $\alpha_s$ , will vanish by applying renormalisation.

yielding  $c_{11} = 1$ .

Beginning from three loop diagrams the algebra becomes exhausting and one has to use dedicated algorithms to compute the higher loops. The third loop calculations have been done in the late seventies by [Chetyrkin1979, Dine1979, Celmaster1979]. The four loop evaluation have been completed a little more than ten years later by [Gorishnii1990, Surguladze1990]. The highest loop published, that amounts to  $\alpha_s^4$ , was published in 2008 [Baikov2008] almost 20 years later.

Fixing the number of colors to  $N_c = 3$  the missing coefficients up to order four in  $\alpha_s$  read:

$$\begin{aligned} c_{2,1} &= \frac{365}{24} - 11\zeta_3 - \left( \frac{11}{12} - \frac{2}{3}\zeta_3 \right) N_f \\ c_{3,1} &= \frac{87029}{288} - \frac{1103}{4}\zeta_3 + \frac{275}{6}\zeta_5 \\ &\quad - \left( \frac{7847}{216} - \frac{262}{9}\zeta_3 + \frac{25}{9}\zeta_5 \right) N_f + \left( \frac{151}{162} - \frac{19}{27}\zeta_3 \right) N_f^2 \\ c_{4,1} &= \frac{78631453}{20736} - \frac{1704247}{432}\zeta_3 + \frac{4185}{8}\zeta_3^2 + \frac{34165}{96}\zeta_5 - \frac{1995}{16}\zeta_7, \end{aligned} \quad (1.2.8)$$

where used the flavor number  $N_f = 3$  for the last line.

The 6-loop calculation has until today not been computed, but Beneke and Jamin [Beneke2008] used an educated guess to estimate the coefficient

$$c_{5,1} \approx 283 \pm 283. \quad (1.2.9)$$

We often see  $c_{5,1}$  applied to estimate the perturbative errors related to missing higher order contributions.

In stating the coefficients  $c_{n,k}$  of the correlator expansion we have restricted ourselves to  $k$  indices equal to one. This is due to the RGE, which relates coefficients with  $k$  different than one to coefficients with  $k$  equal to one ( $c_{n,1}$ ). Consequently the correlator  $\Pi_V^{1+0}(s)$  needs to be a physical quantity, which we can be achieved with the previously defined Adler function (eq. 1.1.7). The correct expression for the correlator expansion in eq. 1.2.4 is then given by

$$D_V^{(1+0)} = -s \frac{d\Pi_V^{(1+0)}(s)}{ds} = \frac{N_c}{12\pi^2} \sum_{n=0}^{\infty} a_\mu^n \sum_{k=1}^{n+1} k c_{n,k} L^{k-1}, \quad (1.2.10)$$

where we used  $dL^k/ds = k \ln(-s/\mu^2)^{k-1} (-1/\mu^2)$ . Applying the RGE (??) to the scale-invariant Adler function yields

$$-\mu \frac{d}{d\mu} D_V^{(1+0)} = -\mu \frac{d}{d\mu} \left( \frac{\partial}{\partial L} D_L + \frac{\partial}{\partial a_s} D_{a_s} \right) D_V^{(1+0)} = \left( 2 \frac{\partial}{\partial L} + \beta \frac{\partial}{\partial a_s} \right) D_V^{(1+0)} = 0, \quad (1.2.11)$$

where we made use of the  $\beta$  function, which is defined in ??, and of the expression  $dL/d\mu = -2/\mu$ .

The relation between the correlator expansion coefficients can then be taken by calculating the Adler function for a desired order and plugging it into the RGE. For example the Adler function to the second order in  $\alpha_s$

$$D(s) = \frac{N_c}{12\pi^2} \left[ c_{01} + a_\mu (c_{11} + 2c_{12}L) + a_\mu^2 (c_{21} + 2c_{22}L + 3c_{23}L^2) \right], \quad (1.2.12)$$

can be inserted into the [eq. 1.2.11](#)

$$4a_\mu c_{12} + 2a_\mu^2 (2c_{22} + 6c_{23}L) + \beta_1 a_\mu^2 (c_{11} + 2c_{12}L) + \mathcal{O}(a_\mu^3) = 0 \quad (1.2.13)$$

to compare the coefficients order by order in  $\alpha_s$ . At order  $\alpha_\mu$  only the  $c_{12}$  term is present and has consequently to be zero. For  $\mathcal{O}(a_\mu^2 L)$  solely  $c_{23}$  exists as  $c_{12} = 0$  and thus also has to vanish. Finally for  $\mathcal{O}(a)$  we can relate  $c_{22}$  with  $c_{11}$  resulting in:

$$c_{12} = 0, \quad c_{22} = \frac{\beta_1 c_{11}}{4} \quad \text{and} \quad c_{23} = 0. \quad (1.2.14)$$

Implementing the newly obtained Adler coefficients we can write out the Adler function to the first order:

$$D(s) = \frac{N_c}{12\pi^2} \left[ c_{01} + c_{11} a_\mu \left( c_{21} - \frac{1}{2} \beta_1 c_{11} L \right) a_\mu^2 \right] + \mathcal{O}(a_\mu^3). \quad (1.2.15)$$

We have used the RGE to relate Adler function coefficients and thus only need to know coefficients of type  $c_{n,1}$ . Unfortunately, as we will see in the following section the RGE gives us two different choices in the order of the computation of the perturbative contribution to the inclusive tau decay ratio.

### Renormalization group summation

By making use of the RGE we have to decide about the order of mathematical operations we perform. As the perturbative contribution  $\delta_{pt}$  is independent on the scale  $\mu$  we are confronted with two choices: *fixed-order perturbation theory*



(FOPT) and *contour-improved perturbation theory* (CIPT). Each of them yields a different result, which is the main source of error in extracting the strong coupling from tau decays.

Working in the chiral limit additionally permits us to neglect the longitudinal contribution  $D^{(0)}$ , in eq. 1.1.13 of the perturbative contribution  $\delta_{\text{pt}}$  of  $R_\tau$  (eq. 1.2.2). Thus inserting the expansion of  $D_V^{(1+0)}$  into the hadronic tau decay width eq. 1.1.13 yields

$$\delta_{\text{pt}} = \sum_{n=1}^{\infty} a_\mu^n \sum_{k=1}^n k c_{n,k} \frac{1}{2\pi i} \oint_{|x|=1} \frac{dx}{x} (1-x)^3 (1+x) \log \left( \frac{-m_\tau^2 x}{\mu^2} \right)^{k-1}, \quad (1.2.16)$$

where we kept in mind that the contributions from the vector and axial-vector correlator are identical in the massless case.

To continue evaluating the perturbative part we can now either follow the description of FOPT or CIPT. We will now present both.

In FOPT we fix the scale at the tau mass ( $\mu^2 = m_\tau^2$ ), which leaves us with the integration over the logarithm, as seen in

$$\delta_{\text{FO}}^{(0)} = \sum_{n=1}^{\infty} a(m_\tau^2)^n \sum_{k=1}^n k c_{n,k} J_{k-1} \quad (1.2.17)$$

where the contour integrals  $J_l$  are defined by

$$J_l \equiv \frac{1}{2\pi i} \oint_{|x|=1} \frac{dx}{x} (1-x)^3 (1+x) \log^l(-x). \quad (1.2.18)$$

The integrals  $J_l$  up to order  $\alpha_s^4$  are given by [Beneke2008]:

$$J_0 = 1, \quad J_1 = -\frac{19}{12}, \quad J_2 = \frac{265}{72} - \frac{1}{3}\pi^2, \quad J_3 = -\frac{3355}{288} + \frac{19}{12}\pi^2. \quad (1.2.19)$$

Using FOPT the strong coupling  $a(\mu)$  is fixed at the tau mass scale  $a(m_\tau^2)$  and can be taken out of the closed-contour integral. Thus we solely have to integrate over the logarithms  $\log(x)$ .

Using CIPT, on the contrary, we can sum the logarithms by setting the scale to  $\mu^2 = -m_\tau^2 x$  in eq. 1.2.16, resulting in:

$$\delta_{\text{CI}}^{(0)} = \sum_{n=1}^{\infty} c_{n,1} J_n^a(m_\tau^2), \quad (1.2.20)$$

where the contour integrals  $J_l$  are defined by

$$J_n^a(m_\tau^2) \equiv \frac{1}{2\pi i} \oint_{|x|=1} \frac{dx}{x} (1-x)^3 (1+x) a^n(-m_\tau^2 x). \quad (1.2.21)$$

Note that all logarithms vanish, except the ones with index  $k = 1$ :

$$\log(1)^{k-1} = \begin{cases} 1 & \text{if } k = 1, \\ 0 & k \neq 1 \end{cases} \quad (1.2.22)$$

which selects the Adler function coefficients  $c_{n,1}$ . Handling the logarithms left us with the integration of the strong coupling  $\alpha_s(-m_\tau^2 x)$  over the closed-contour  $\oint_{|x|=1}$ , which now depends on the integration variable  $x$ .

In general we have to decide if we want to perform a contour integration with a constant strong coupling parameter and variable logarithms (FOPT) or “constant logarithms” and a running coupling (CIPT). To emphasize the differences in both approaches we can calculate the perturbative contribution  $\delta^{(0)}$  to  $R_\tau$  for the two different prescriptions yielding [Beneke2008]

$$\begin{aligned} & \alpha_s^2 \quad \alpha_s^2 \quad \alpha_s^3 \quad \alpha_s^4 \quad \alpha_s^5 \\ \delta_{\text{FO}}^{(0)} &= 0.1082 + 0.0609 + 0.0334 + 0.0174(+0.0088) = 0.2200(0.2288) \end{aligned} \quad (1.2.23)$$

$$\delta_{\text{CI}}^{(0)} = 0.1479 + 0.0297 + 0.0122 + 0.0086(+0.0038) = 0.1984(0.2021). \quad (1.2.24)$$

The series indicate, that CIPT converges faster and that both series approach a different value. This discrepancy represents currently the biggest theoretical uncertainty for extracting the strong coupling.

As today FOPT or CIPT are equally valid approaches to calculate the perturbative contributions. As a result there are currently three ways of stating results: Quoting the average of both results, quoting the CIPT result or quoting the FOPT result. We follow the approach of Beneke and Jamin [Beneke2008] who prefer FOPT, but also state their results in CIPT.

### 1.2.2 The Non-Perturbative OPE Contributions

The perturbative contribution to the sum rule is the dominant one, but NP have to be taken into account. The contribution of the NP part can be quoted as

$$\delta_{\text{NP}} = 0,007 \pm 0.004 \quad [\text{Braaten1991}], \quad (1.2.25)$$

which is small, but not negligible. The NP OPE contributions are commonly categorised by even, increasing dimensions. Contributions of dimension larger

than eight are normally neglected, due to the increasing suppression by factors of  $1/m_\tau^{2 \cdot D}$ , where  $D$  stands for the corresponding dimension.

The dimension two contributions are proportional to the quark masses and vanish while working in the chiral limit. Consequently we will neglect them and start by stating the  $D = 4$  contributions.

### 1.2.3 Dimension four

**write more details** The next apparent OPE contribution is of dimension four. Here we have to take into account the terms with masses to the fourth power ( $m^4$ ), the quark condensate multiplied by a mass ( $m\langle\bar{q}q\rangle$ ) and the gluon condensate ( $\langle GG\rangle$ ). The resulting expression can be taken from the appendix of [Pich1999], yielding:

$$D_{ij}^{(1+0)}(s)\Big|_{D=4} = \frac{1}{s^2} \sum_n \Omega^{(1+0)}(s/\mu^2) a^n, \quad (1.2.26)$$

where

$$\begin{aligned} \Omega_n^{(1+0)}(s/\mu^2) = & \frac{1}{6} \langle aGG \rangle p_n^{(1+0)}(s/\mu^2) + \sum_k m_k \langle \bar{q}_k q_k \rangle r_n^{(1+0)}(s/\mu^2) \\ & + 2 \langle m_i \bar{q}_i q_i + m_j \bar{q}_j q_j \rangle q_n^{(1+0)}(s/\mu^2) \pm \frac{8}{3} \langle m_j \bar{q}_i q_i + m_i \bar{q}_j q_j \rangle t_n^{(1+0)} \\ & - \frac{3}{\pi^2} (m_i^4 + m_j^4) h_n^{(1+0)}(s/\mu^2) \mp \frac{5}{\pi^2} m_i m_j (m_i^2 + m_j^2) k_n^{(1+0)}(s/\mu^2) \\ & + \frac{3}{\pi^2} m_i^2 m_j^2 g_n^{(1+0)}(s/\mu^2) + \sum_k m_k^4 j_n^{(1+0)}(s/\mu^2) + 2 \sum_{k \neq l} m_k^2 m_l^2 u_n^{(1+0)}(s/\mu^2) \end{aligned} \quad (1.2.27)$$

The perturbative expansion coefficients are known to  $\mathcal{O}(a^2)$  for the condensate contributions,

$$\begin{aligned} p_0^{(1+0)} &= 0, & p_1^{(1+0)} &= 1, & p_2^{(1+0)} &= \frac{7}{6}, \\ r_0^{(1+0)} &= 0, & r_1^{(1+0)} &= 0, & r_2^{(1+0)} &= -\frac{5}{3} + \frac{8}{3} \zeta_3 - \frac{2}{3} \log(s/\mu^2), \\ q_0^{(1+0)} &= 1, & q_1^{(1+0)} &= -1, & q_2^{(1+0)} &= -\frac{131}{24} + \frac{9}{4} \log(s/\mu^2) \\ t_0^{(1+0)} &= 0, & t_1^{(1+0)} &= 1, & t_2^{(1+0)} &= \frac{17}{2} + \frac{9}{2} \log(s/\mu^2). \end{aligned} \quad (1.2.28)$$

while the  $m^4$  terms have been only computed to  $\mathcal{O}(\alpha)$

$$\begin{aligned}
 h_0^{(1+0)} &= 1 - 1/2 \log(s/\mu^2), & h_1^{(1+0)} &= \frac{25}{4} - 2\zeta_3 - \frac{25}{6} \log(s/\mu^2) - 2 \log(s/\mu^2)^2, \\
 k_0^{(1+0)} &= 0, & k_1^{(1+0)} &= 1 - \frac{2}{5} \log(s/\mu^2), \\
 g_0^{(1+0)} &= 1, & g_1^{(1+0)} &= \frac{94}{9} - \frac{4}{3} \zeta_3 - 4 \log(s/\mu^2), \\
 j_0^{(1+0)} &= 0, & j_1^{(1+0)} &= 0, \\
 u_0^{(1+0)} &= 0, & u_2^{(1+0)} &= 0.
 \end{aligned} \tag{1.2.29}$$

#### 1.2.4 Dimension six and eight

Our application of dimension six contributions is founded in [Braaten1991] and has previously been calculated beyond leading order by [Lanin1986]. The operators appearing are the masses to the power six ( $m^6$ ), the four-quark condensates ( $\langle \bar{q} q \bar{q} q \rangle$ ), the three-gluon condensates ( $\langle g^3 G^3 \rangle$ ) and lower dimensional condensates multiplies by the corresponding masses, such that in total the mass dimension of the operator will be six. The largest contributions comes from the 4-quark operators. The three-gluon condensate does not contribute at leading order [Hubschmid1982] and is neglected. Operators proportional to the light quark masses will also be neglected. The resulting contribution of dimension six operators has been calculated in [Laning1986] and leads to a large amount of operators, which until today cannot be accurately determined by phenomenology methods. To reduce the number of operators we can make use of the *vacuum saturation approach* (vsa) [Beneke2008, Braaten1991, Shifman1978] to express them in quark condensates  $\langle q \bar{q} \rangle$ . For Wilson coefficients of order  $\alpha_s$  and applying the vacuum saturation we get a dimension six contributions of

$$D_{ij,V/A}^{1+0}(s) \Big|_{D=6} = \frac{32\pi^2}{3} a(\mu) \frac{\langle \bar{q}_i q_i(\mu) \rangle \langle \bar{q}_j q_j \rangle}{s^3} - \frac{32}{7} \pi^2 a_\mu \frac{\langle \bar{q}_i q_i \rangle^2 \langle \bar{q}_j q_j \rangle^2}{s^3}. \tag{1.2.30}$$

Unfortunately the scaling properties of the dimension six contribution, resulting from the vsa, are inconsistent with the scaling properties of the 4-quark operators [Narison1983, Jamin1985] and terms of order  $\alpha_s^2$  are usually ignored. In addition to the scaling problematic the vsa is known to underestimate the dimension six contribution [Launer1983].

In our work we take the simplest approach possible: Introducing an effective

dimension six coefficient  $\rho_{V/A}^{(6)}$  divided by the appropriate power in  $s$

$$D_{ij,V/A}^{(1+0)}(s) \Big|_{D=6} = 0.03 \frac{\rho_{V/A}^{(6)}}{s^3} \quad (1.2.31)$$

As for the dimension eight contribution the situation is not better than the dimension six one we keep the simplest approach, leading to

$$D_{ij,V/A}^{(1+0)} \Big|_{D=8} = 0.04 \frac{\rho_{V/A}^{(8)}}{s^4}. \quad (1.2.32)$$

The NP contribution of dimension eight is the highest order that we are going to implement. Higher orders will be neglected. Next to the NP treatment of the OPE we also have to discuss possible duality violations.

### 1.3 Duality Violations

As seen in ?? we have to assume quark-hadron duality for the QCDSR to work. Unfortunately duality cannot always be taken for granted and the existence of *duality violations* (DV) is a well known [Cat2008, Cat2009]. As we will see in the following section, the experimental measured total tau decay ratio has a exponential decreasing, sinusoidal contributions, that cannot be reproduced by the OPE solely. Consequently for the cases with apparent DV we also have to take into account DV corrections and adapt eq. 1.2.2

$$R_{\tau,V/A}^{\omega} = \frac{N_c}{2} S_{EW} |V_{ud}|^2 \left( 1 + \delta_{pt}^{\omega} + \delta_{npt}^{\omega} + \delta_{dv}^{\omega} \right). \quad (1.3.1)$$

The DV correction has been modelled by a series of papers [Boito2011a, Boito2012, Boito2014] with the following ansatz

$$\rho_{V/A}^{DV}(s) = e^{-(\delta_{V/A} + \gamma_{V/A}s)} \sin(\alpha_{V/A} + \beta_{V/A}s), \quad (1.3.2)$$

to parametrise the DV contributions. The DV would then appear as an additional term in the inclusive tau decay ratio

$$R_{\tau,V/A} = -\pi i \oint_{|s|=m_{\tau}^2} \frac{dx}{x} (1-x)^3 \left[ 3(1+x) D^{(1+0)}(m_{\tau}^2 x) + 4 D^{(0)}(m_{\tau}^2 x) \right] + \mathcal{D}_{V/A}(m_{\tau}^2), \quad (1.3.3)$$

where the DV would be given as

$$\mathcal{D}_{\omega}(m_{\tau}^2) = -12\pi^2 \int_{m_{\tau}^2}^{\infty} \frac{ds}{m_{\tau}^2} \omega(s) \rho_{V/A}. \quad (1.3.4)$$

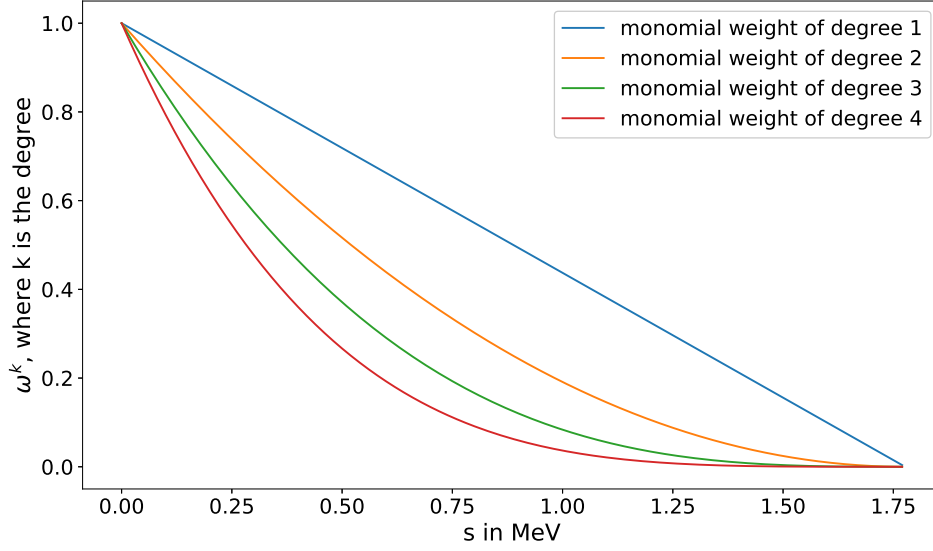


Figure 1.2: Monomial weights  $(1 - s/m_\tau^2)^k$  for degrees  $1 \rightarrow 4$ . We can see that weights of higher pinching decrease faster, which comes in handy if we want to suppress duality violations.

### 1.3.1 Pinched weights to avoid DVs

The general QCDSR (??) contain a weight function  $\omega$ , which is used to weight higher order dimensions, but also to suppress dv. The weights that suppress dv are so-called pinched weights of the form

$$\omega(s) = \left(1 - \frac{s}{m_\tau^2}\right)^k, \quad (1.3.5)$$

where  $k$  is the degree of the pinched weight. The higher the degree the farther we operate from the critical positive real axis (see. ??). The farther we are away the better we are protected from the effects of dv. For the transversal component of the inclusive tau decay ratio (eq. 1.1.2) a pinching of second degree appears quite naturally as the kinematic weight (see ??).

In general it is said that a double pinched weight is sufficient to neglect effects caused by duality violation.

Next to the pinched weights we focus on combinations of vector and axial-vector contributions, which as we will see now suppress dv.

## 1.4 Experiment

The tau decay data we use to perform our QCD analysis is from the ALEPH experiment. The ALEPH experiment was located at the *large-electron-positron* (LEP) collider at *European Organisation for Nuclear Research* (CERN) in Geneva. LEP started producing particles in 1989 and was replaced in the late 90s by the *large-hadron-collider* (LHC), which makes use of the same tunnel of 27 km circumference. The data produced within the experiment is still maintained by former ALEPH group members led by M. Davier, which have performed regular updates on the data-sets [Davier2013, Davier2008, Aleph2005].

The measured spectral functions for the ALEPH data are defined in [Davier2007] and given for the transverse and longitudinal components separately

$$\begin{aligned}\rho_{V/A}^{(1)}(s) &= \frac{m_\tau^2}{12|V_{ud}|^2 S_{EW}} \frac{\mathcal{B}(\tau^- \rightarrow V^-/A^- \nu_\tau)}{\mathcal{B}(\tau^- \rightarrow e^- \bar{\nu}_e \nu_\tau)} \\ &\quad \times \frac{dN_{V/A}}{N_{V/A} ds} \left[ \left(1 - \frac{s}{m_\tau^2}\right)^2 \left(1 + \frac{2s}{m_\tau^2}\right) \right]^{-1} \\ \rho_A^{(0)}(s) &= \frac{m_\tau^2}{12|V_{ud}|^2 S_{EW}} \frac{\mathcal{B}(\tau^- \rightarrow \pi^- (K^-) \nu_\tau)}{\mathcal{B}(\tau^- \rightarrow e^- \bar{\nu}_e \nu_\tau)} \times \frac{dN_A}{N_A ds} \left(1 - \frac{s}{m_\tau^2}\right)^{-2}.\end{aligned}\tag{1.4.1}$$

The data relies on a separation into vector and axial-vector channels. In the case of the pions this can be achieved via counting. The vector channel is characterised by a negative parity, whereas the axial-vector channel has positive parity. A quark has by definition positive parity, thus an anti-quark has a negative parity. A meson, like the pion particle, is a composite particle consisting of an quark an anti-quark. Consequently a single pion carries negative parity, an even number of Pions carries positive parity and an odd number of Pions carries negative parity:

$$n \times \pi = \begin{cases} \text{vector} & \text{if } n \text{ is even,} \\ \text{axial-vector} & \text{otherwise} \end{cases}.\tag{1.4.2}$$

The contributions to the spectral function for the vector, axial-vector and V+A channel can be seen in fig. 1.3. The dominant modes in the vector case are [Davier2006]  $\tau^- \rightarrow \pi^- \pi^0 \nu_\tau$  and the  $\tau^- \rightarrow \pi^- \pi^- \pi^+ \pi^0 \nu_\tau$ . The first of these is produced by the  $\rho(770)$  meson, which in contrary to the pions carries angular momentum of one, which is also clearly visible as peak around 770 GeV in

fig. 1.3a. The dominant modes in the axial-vector case are  $\tau^- \rightarrow \pi^- \nu_\tau$ ,  $\tau^- \rightarrow \pi^- \pi^0 \pi^0 \nu_\tau$  and  $\tau^- \rightarrow \pi^- \pi^- \pi^+ \nu_\tau$ . Here the three pion final states stem from the  $a_1^-$ -meson, which is also clearly visible as a peak in fig. 1.3b.

We furthermore added the perturbative result for a fixed  $\alpha_s(m_\tau) = 0.329$  using FOPT in fig. 1.3c. Here we can see, that the perturbative result (the blue line) is an almost straight line and cannot reproduce the sinusoidal graph, given by the ALEPH data. This is especially the case for the v and A channel and is seen as an indicator for DV. Even including NP, higher dimensions of the OPE is not reproducing the wavy structure. In the case of v+A, we have a higher agreement between our perturbative graph and the data. In general we believe that DV are sufficiently suppressed in the case of v+A and will argue in favour of this statement in the following chapter. This is only the case for energies larger than 1.5 GeV, as the  $\rho$  resonance of the v channel is impossible to be represented by perturbative tools. For lower energies DV become too important to be neglected.

#### 1.4.1 Total decay ratio from experimental data

The data has been last revised in 2014 [Davier2014] and is publicly available [AlephData]. It consists of the mass squared bin center  $s_{bin}$ , the bin size  $ds_{bin}$ , the normalised invariant mass squared distribution  $s_{fm2}$ , the total errors  $derr$  and their correlations  $corerr$ . To make the data comparable to our theoretical calculations we have to give the normalised invariant mass squared distribution  $s_{fm2}$  in form of the total decay ratio  $R_\tau$ . The data is given as the normalised invariant mass squared distribution  $(dN_i/ds)/N_i$  scaled by a factor 100 and further normalised to the corresponding branching ratio  $i \in \{V, A, V+A\}$ . Thus we can connect the branching ratio of the i-channel to  $s_{fm2}$  as follows

$$\mathcal{B}_{V/A} \equiv \int_0^{s_\tau} ds \frac{s_{fm2_{V/A}(s)}{100}}{100} \equiv \int_0^{s_\tau} ds \mathcal{B}_{V/A} \left( \frac{dN_{V/A}}{N_{V/A} ds} \right) \quad (1.4.3)$$

where we defined  $s_\tau \equiv m_\tau^2$ . The total decay ratio  $R_\tau$  is defined as the decay width of taus decaying into hadrons over taus decaying into electrons and can be expressed via the corresponding branching ratios, which then can be



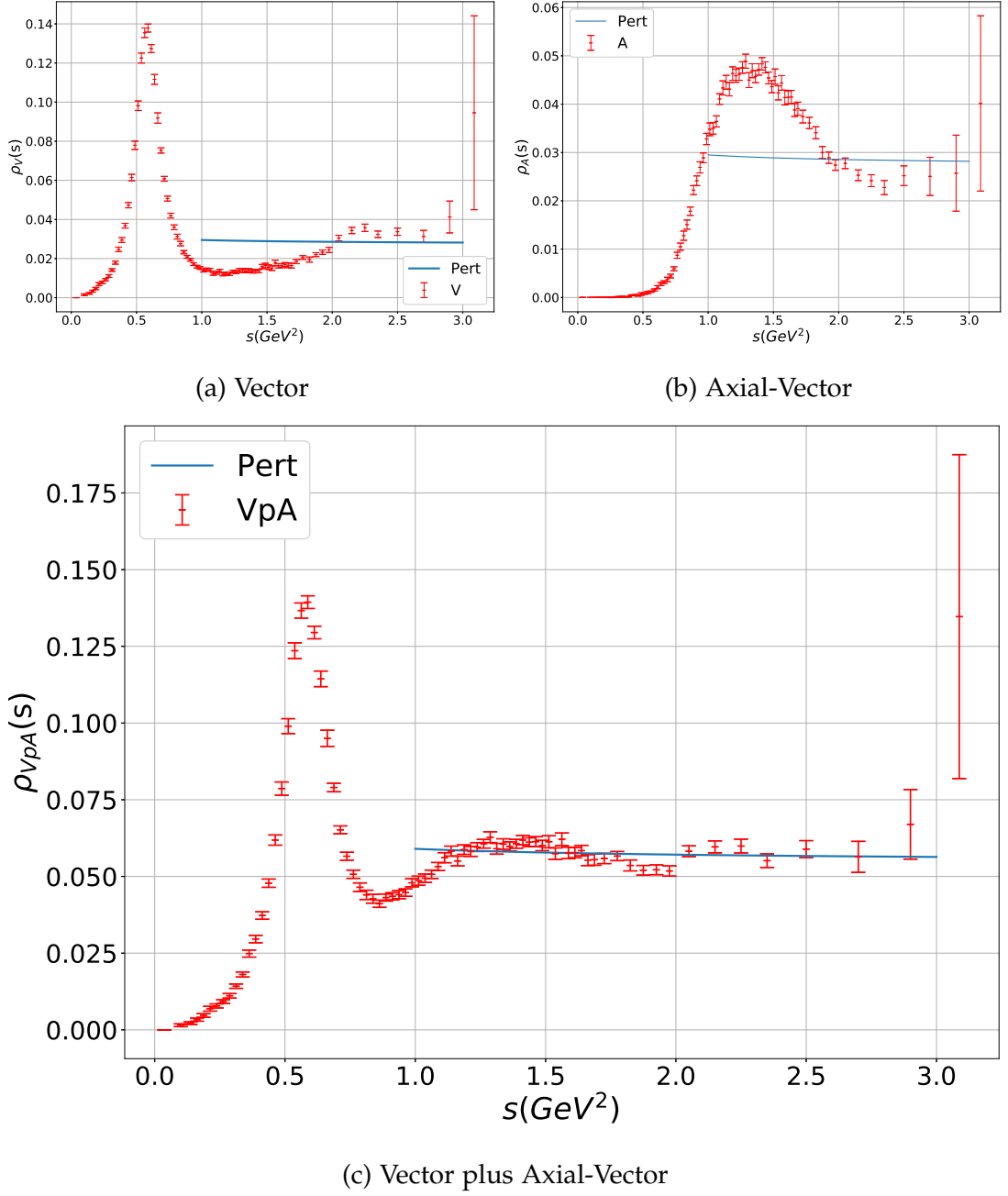


Figure 1.3: Visualisation of the vector, axial-vector and V+A spectral function given by the ALEPH data [Davier2013] in red with errors. We also plotted the FOPT theoretical calculation up to third order in  $\alpha_s$ , for a fixed  $\alpha_s(\tau) = 0.329$  in blue. Note that the perturbative contribution can only limited represent the experimental data. It does not reproduce the sinusoidal form.

connected to the invariant mass squared distribution  $\text{sfm2}$

$$R_{\tau,V/A} = \frac{\mathcal{B}_{V/A}}{\mathcal{B}_\parallel} = \int_0^{s_\tau} ds \frac{\text{sfm2}_{V/A}(s)}{100\mathcal{B}_e}. \quad (1.4.4)$$

Theoretically the decay ratio is given in ???. If we neglect the longitudinal contribution  $\text{Im}\Pi^{(0)}(s)$  and remember the definition of the spectral function (??) and the kinematic weight (??), we can write the decay ratio as

$$R_{\tau,i} = \int_0^{s_\tau} \frac{ds}{s_\tau} \omega_\tau(s) \rho(s) \quad (1.4.5)$$

and thus relate the spectral function to the experimental data

$$\rho(s) = \frac{s_\tau}{12\pi^2 100\mathcal{B}_e} \frac{\text{sfm2}}{\omega_\tau}. \quad (1.4.6)$$

To fit the experimental data we define a so-called *spectral function moment* (or *moment*)

$$I_i^{\text{exp},\omega} \equiv \int_0^{s_0} \frac{ds}{s_0} \omega\left(\frac{s}{s_0}\right) \rho(s), \quad (1.4.7)$$

which will be used in our  $\chi^2$  fits, explained in the upcoming section. The data is given for discrete bins so we have to express the integral of the spectral function moment as sum over those bins. The final expression we use to fit parameters to the experimental data is then given by

$$I_{\text{exp},V/A}^\omega(s_0) = \frac{s_\tau}{100\mathcal{B}_e s_0} \sum_{i=1}^{N(s_0)} \frac{\omega\left(\frac{s_i}{s_0}\right)}{\omega_\tau\left(\frac{s_i}{s_\tau}\right)} \text{sfm2}_{V/A}(s_i). \quad (1.4.8)$$

## 1.5 The Method of Least Squares

We apply *method of least squares* (LS) to fit the parameters  $\vec{\alpha}$  from the experimental data. We consequently construct a  $\chi^2$ -function

$$\chi^2 = \left( I_i^{\text{exp}} - I_i^{\text{th}}(\vec{\alpha}) \right) C_{ij}^{\text{exp}-1} \left( I_j^{\text{exp}} - I_j^{\text{th}}(\vec{\alpha}) \right), \quad (1.5.1)$$

where  $I^{\text{exp}} / I^{\text{th}}$  is a vector of experimental moments/ theoretical moments with the same weight, but different energy cutoffs  $s_0$ , labelled by the index  $i$ . In addition  $C^{\text{exp}}$  is the covariance matrix describing the correlation of the

different experimental moments  $C_{ij}^{\text{exp}} = \text{cov}[I_i^{\text{exp}}, I_j^{\text{exp}}]$ , which is given by the ALEPH data.

In general we aim to minimise the value of  $\chi^2$ , which will fix the parameter vector  $\vec{\alpha}$ . The properties of the  $\chi^2$ -function are well known and the best fits are characterised through  $\chi^2/\text{dof} \approx 1$ , where the DOF of the fit can be calculated through

$$\text{DOF} = \text{experimental moments} - \text{parameters}. \quad (1.5.2)$$

E.g. if we want to fit  $\alpha_s$  and the dimension four Wilson coefficient  $C_4$  we get  $7 - 2 = 5$  DOF.

The parameter vector  $\vec{\alpha}$  includes the strong coupling  $\alpha_s$ , but also the included OPE Wilson coefficient. Consequently we should have at least as many, if not more moments as parameters we want to fit. As the moments for different  $s_0$  are highly correlated we are limited to fit a set of only a few parameters.

It is also possible to increase the number of moments used by using multiple weights  $\omega$ . Unfortunately using different weights leads to highly correlated moments, which leads to numerical complications by inverting the covariance matrix in [eq. 1.5.1](#). To handle the high correlations we have to redefine our fit quality.

### 1.5.1 Block Diagonal “Fit-Quality”

Following [\[Boito2014\]](#) we can redefine LS to

$$Q^2 = \sum_{\omega} \sum_{s_0^i, s_0^j} \left( I_{\omega}^{\text{exp}}(s_0^i) - I_{\omega}^{\text{th}}(s_0^i, \vec{\alpha}) \right) \tilde{C}_{ij, \omega}^{-1} \left( I_{\omega}^{\text{exp}}(s_0^j) - I_{\omega}^{\text{th}}(s_0^j, \vec{\alpha}) \right), \quad (1.5.3)$$

where the covariance matrix  $\tilde{C}$  is now a diagonal of the experimental covariance matrices  $C_{\omega}^{\text{exp}}$  for each weight

$$\tilde{C} = \begin{pmatrix} C_{\omega=1}^{\text{exp}} & 0 & \dots & 0 \\ 0 & C_{\omega=2}^{\text{exp}} & \ddots & \vdots \\ \vdots & \ddots & \ddots & 0 \\ 0 & \dots & 0 & C_{\omega=n}^{\text{exp}} \end{pmatrix}. \quad (1.5.4)$$

As a result we are still able to invert the newly defined covariance matrix  $\tilde{C}$ ,

but minimisation routines like CERN MINUIT are now able to calculate the proper errors for the parameters we want to extract. We have to perform our own error propagation to obtain meaningful errors for the parameters.

### Error Propagation

The error propagation has been derived in [Boito2011a, Boito2011] and is given as

$$\langle \delta\alpha_k \alpha_l \rangle = A_{km}^{-1} A_{ln}^{-1} \frac{\partial I_i^{\text{th}}(\vec{\alpha})}{\partial \alpha_m} \frac{\partial I_r^{\text{th}}(\vec{\alpha})}{\partial \alpha_n} \tilde{C}_{ij}^{-1} \tilde{C}_{ij}^{-1} \langle \delta I_k^{\text{exp}} \delta I_l^{\text{exp}} \rangle, \quad (1.5.5)$$

where

$$A_{kl} = \frac{\partial I^{\text{th}}(\vec{\alpha})}{\partial \alpha_k} C_{ij}^{-1} \frac{I_j^{\text{th}}(\vec{\alpha})}{\alpha_l}. \quad (1.5.6)$$